

Detection of candidate primordial galaxies at $z > 4$ *

V. Le Brun¹, J. Boulesteix², A. Mazure¹, P. Amram², G. Courtès²

¹ IGRAP, Laboratoire d'Astronomie Spatiale du C.N.R.S., B.P. 8, F-13376 Marseille CEDEX 12, France, lebrun@lasa13.astrsp-mrs.fr, mazure@astrsp-mrs.fr

² IGRAP, Observatoire de Marseille, 2 Place Le Verrier, F-13248 Marseille CEDEX 04, France, boulesteix@obmara.cnrs-mrs.fr, amram@obmara.cnrs-mrs.fr

Received November 1997; accepted ?

Abstract. We report on the detection of four primordial galaxies candidates in the redshift range $4.55 \leq z \leq 4.76$, as well as 4 other candidates in the range $4.12 \leq z \leq 4.32$. These galaxies have been detected with the now common technique of the Lyman break, but with a very original instrumental setup, which allows the simultaneous detection on a single exposure of three narrow (FWHM ~ 200 Å) bands. Depending on between which pair of bands the Lyman break is located, it thus allows to detect two ranges of redshifts. Two of the the higher redshift candidates are located only $50h_{50}^{-1}$ kpc apart, thus forming a possible primordial galaxy pair.

Key words: quasar: absorption lines – galaxies: ISM – galaxies: halos

1. Introduction

The knowledge of the epoch when galaxies formed, that is when they formed the bulk of their stars, is a major cosmological question. The detection of such primordial galaxies would give constraints on their formation, their chemical evolution or the formation of large scale structures. All the attempts to detect these galaxies at redshifts $z \geq 3$ by detecting the Ly α emission line, either by visible and IR spectroscopy (Koo & Kron 1980, Schneider et al. 1991, Thompson & Djorgovski 1995), narrow band imaging (De Propriis et al. 1993, Parkes et al. 1994) or Perot-Fabry (Thompson et al. 1995) have failed, while the Ly α flux of a $z = 4$ galaxy, $\sim 10^{-16 \pm 1}$ erg cm⁻² s⁻¹ (Thompson & Djorgovski 1995), should have been easily observed with 3.6m telescopes. Only recently, Hu (1998) reported the detection of Ly α emitters at redshifts as high as 4.5. However, it is now known that even small amounts of dust can absorb the great majority of the Ly α photons by resonant scattering (Charlot & Fall 1993).

The most promising method to observe these galaxies seems to use the Lyman break at 912 Å. This break

is present in all kinds of galaxies, for all reasonable stellar formation scenarii (Bruzual & Charlot 1993), and is observed in the visible range for $z \geq 3.5$.

The first very high redshift galaxies have been observed through multi band imaging, with broad filters located on each side of the Lyman break at $\langle z \rangle = 3.2$, selected using color criteria, and several of the candidates have recently been spectroscopically confirmed with the Keck telescope (Steidel & Hamilton 1992,1993, Steidel et al. 1995, Pettini et al. 1997). The average projected density of these objects is expected to be 0.5 gal arcmin⁻² at $R \sim 25$ and $\langle z \rangle = 3.2$ (Steidel et al. 1995).

In this paper, we present the results of the search for very high redshift galaxies ($z \sim 4.5$), using the same technique, but with an original instrumental setup : we have designed multi band filters, with three narrow (FWHM $\simeq 200$ Å) bands, placed so that they avoid the most prominent night sky emission lines. This disposition and the very high transmission (above 95%) of the filters compensate the narrowness of the bands, and reduces by a factor of three the amount of data to reduce, as well as telescope observing time.

Observations are described in Sect. 2, and our detections are discussed in Sect. 3.

2. Observations and data reduction

We have observed the field #F of the Calar Alto Deep Imaging Survey (Hippelein et al. 1995), centered at position 13h 47m 42.1s +05 deg 37'35.6" (J2000). The CADIS fields have been selected for being empty of bright stars or galaxies. Observations were carried at the ESO 3.6m Telescope at la Silla between the 2nd and the 5th of April 1997, with EFOOSC. The Tektronik CCD has a 0.61" pixel size.

We have taken two exposures of the field : one in the standard R filter, so that we could locate precisely the objects and measure their magnitude, and one with the 3-band filter, to detect their Lyman edge. The full instrumental setup and properties are described in Boulesteix et al. (1997). In short, the three bands have been designed to avoid the most prominent night sky emission lines (5700 Å,

Send offprint requests to: V. Le Brun

* Based on observations made with the ESO 3.6m Telescope

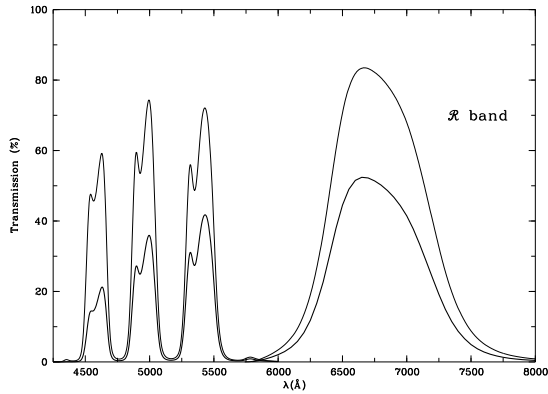


Fig. 1. Transmission curves of the optical device alone (multi-band filter and prisms, thin curve), and of the overall setup (optical device, EFOSC and CCD, thick curve)

6003 Å), so that the background noise is significantly reduced. The bandpass of the multi-band filter is shown on the left part of Fig. 1, while the right part of this figure gives the transmission of the R filter. We both show the transmission of the optical device (filter + prisms or R filter), and the curve obtained when including the transmissions of the prisms, the multi-band filter and the broad band filter that is used to avoid transmission outside the desired wavelength range (due to residual transmission of the multi band filter below 4450 Å and above 5600 Å), and EFOSC and CCD efficiencies. We have checked that the optical device does not induce any distortion from center to edge of the field, neither in photometry nor in the relative locations of the three images of a given object.

The separation of the images in the 3 bands of our filter, $2.7''$, has been calculated to avoid crowding with the closest objects on the sky and is close to the limit resolution of the telescope and seeing. It assures an almost gaussian image without overlap of the images. The average projected density of galaxies with apparent magnitude below $m_R = 25$ is given by the integration of the differential magnitude-number counts of field galaxies given by e.g. Le Brun et al. (1993):

$$\frac{\partial^2 N}{\partial S \partial m} = 10^{(0.366 \pm 0.01)m_R - (4.24 \pm 0.31)} \text{deg}^{-2}, \quad (1)$$

in very good agreement with those obtained by Metcalfe et al. (1991), Smail et al. (1995) or Driver et al. (1994). This gives an average distance between galaxies of about $10''$. Thus, with the two extreme images separated by $5.8''$, we avoid crowding in a large majority of cases.

The flat fields were made by averaging all the exposure in the same filter (R or multi-band), and the final image was reconstructed by using the shift-and-add procedure. The total exposure time is thus 2 hours in the R band and 10 hours in the multi-band filter and the final field of view, reduced by vignetting and shift-and-add procedure, is $4'50''$ square. Detection of the objects on the R expo-

Table 1. Characteristics of the candidates

Object	m_R	F(6800)	F(5400)	F(4950)	F(4590)
		(10 ⁻¹⁹ erg cm ⁻² s ⁻¹ Å ⁻¹)			
High redshift candidates ($4.55 \leq z \leq 4.76$)					
H1	24.5	2.71 ± 0.8	4.03 ± 0.63	≤ 1.10	≤ 1.50
H2	23.8	5.18 ± 1.0	4.56 ± 0.63	≤ 1.10	≤ 1.50
H3	24.3	3.26 ± 0.6	4.54 ± 0.53	≤ 1.01	≤ 1.37
H4	24.1	3.92 ± 0.8	6.68 ± 0.63	≤ 1.10	≤ 1.50
Low redshift candidates ($4.12 \leq z \leq 4.32$)					
L1	23.8	5.17 ± 0.6	4.77 ± 0.63	5.15 ± 1.10	≤ 1.50
L2	24.2	3.58 ± 0.5	6.68 ± 0.53	4.97 ± 0.91	≤ 1.25
L3	24.3	3.26 ± 0.6	4.77 ± 0.53	4.42 ± 0.91	≤ 1.25
L4	23.9	4.72 ± 1.0	2.76 ± 0.47	3.50 ± 0.83	≤ 1.13
Emission line object					
E1	23.7	5.89	4.63 ± 0.6	14.82 ± 1.1	7.37 ± 1.5

sure was carried using the SExtractor software (Bertin & Arnouts 1996). Thus, knowing the position of all the objects on the field, we have performed aperture magnitude, in a $2''$ box, of the three images of each object on the 3-band filter exposure, at the expected location of each image. We have verified on objects for which the three images were detected that our expectation of the location of the images was correct. Photometric and flux calibrations were made in the R band using the field Ser 1 (Tyson 1988), and the calibration of the multi-band filter exposures was made using the spectrophotometric standard star Kopff 27 (Stone 1977).

For our search of very high redshift galaxies, we have selected objects with apparent magnitude in the range $23.5 \leq m_R \leq 25$. The lower limit corresponds to objects for which the three images are severely blended (due to the large pixel size), and the upper limit to the limiting magnitude of the R image. Thereafter, we have selected, among the 352 objects in this magnitude range, those for which the image quality was good enough to perform photometry of the three images. We note however that blending of objects with each other was in our case less a crucial problem than the blending between the three images of an individual object due to the large pixel size of the EFOSC CCD. We then come up with a list of 88 objects, for which we could perform efficient photometry. We have thus verified, using Kolmogorov-Smirnov test, that this selection did not introduce any bias in the spatial distribution of the objects, and in fact neither the abscissa nor ordinate distribution of the selected objects do deviate significantly from an uniform distribution.

Among these objects, four show image neither in the intermediate nor in the bluer band, and are thus candidates for being galaxies in the redshift range $4.55 \leq z \leq 4.76$, and four more show only two images in the two redder bands, thus being potentially at redshifts in the range $4.12 \leq z \leq 4.32$.

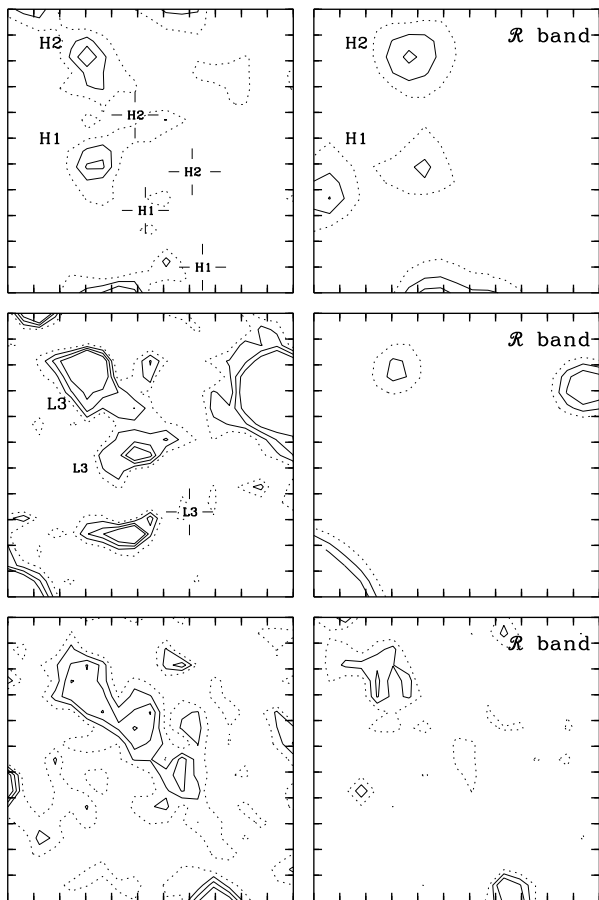


Fig. 2. Images of different types of objects. Upper panel shows the two close higher redshift candidates H1 and H2, intermediate panel shows the $4.13 \leq z \leq 4.38$ candidate L3, and the lower panel shows an object of comparable magnitude which shows the three band in emission, for comparison sake. The dispersion direction goes from top-left to down-right, with decreasing wavelength. The symbols at the center of the crosses indicate the expected location of the blue image(s)

3. Results and discussion

We present in Table 1 the characteristics of the candidates, for both redshift ranges. The R magnitude is given in Column 2, and the calibrated fluxes (or the limits) in the Columns 3 to 6.

3.1. The higher redshift candidates

Upper panel of Fig. 2 presents the four galaxies candidates at redshifts $4.55 \leq z \leq 4.83$, both in R band and in the multi-band filter image. For these four objects, the flux in the intermediate band is at least 3.7 times smaller than expected, if the flux had a flat distribution.

The main concern in such a photometric study is the possible contamination by lower redshift objects, whose spectra show strong features (e.g. ellipticals), that can

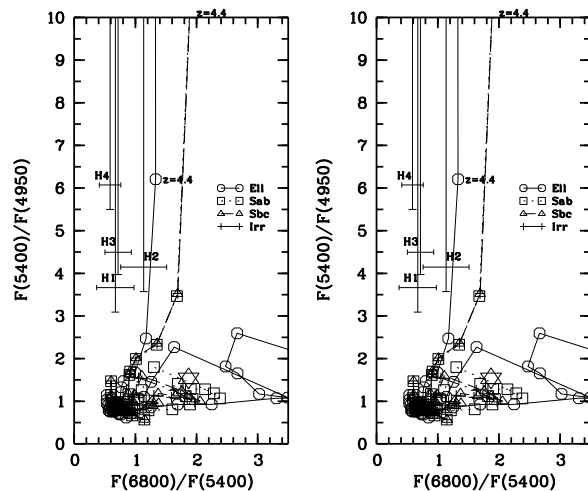


Fig. 3. Color-color diagram for the highest redshift candidates. $F(6800)$ denotes the flux in the R band, while $F(5400)$ and $F(4950)$ are the fluxes in the two redder bands of the multiband filter. The location of our four candidates, with the 3σ error bars, is also shown. The left diagram is for a high value of the intergalactic transmission, right plot for an average transmission. The star-like symbols show the colors of an M type star

produce the same effects that very high redshift galaxies. Thus, in the same way as Steidel et al. (1995), we have simulated the evolutions of the colors of different standard types of galaxies for all redshifts between 0 and 5. The results for the colors relevant for the high redshift objects (namely $F(5400)/F(4950)$ vs $F(6800)/F(5400)$) are given in Fig. 3. We have included in the simulations the effect of the absorption by the intergalactic medium (the so-called Ly α forest), following the prescription of Madau (1995), specifically his Figure 3. As can be seen from this figure, the Universe is transparent above the redshifted wavelength of the Ly α line, and totally opaque below the redshifted Lyman limit. The absorption between these values is very uncertain, due to the statistical fluctuation of the number of absorbers toward a particular sightline. We thus have performed several simulations with various values and form of the intergalactic absorption. We show two of them, corresponding to the average and highest transmission curve. As can be seen, the only effect of a stronger Ly α forest absorption is to make all objects redder in $F(6800)/F(5400)$, but does not modify by a significant amount the $F(5400)/F(4950)$, since both bands are affected in the same proportion. Thus, the value of $F(5400)/F(4950)$ alone can be used to detect very high redshift galaxy candidates, since a galaxy of any type at lower redshift cannot reproduce the observed colors. As well, faint M stars do not have colors compatible with those of high redshift galaxies.

Thus, in the hypothesis that these objects are at redshift above 4.5, objects H1 and H2 are located $3.6''$ apart

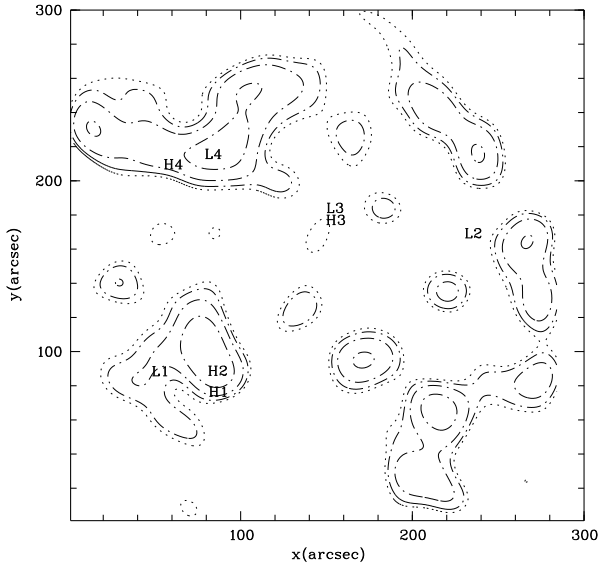


Fig. 4. Galaxy density map of the CADIS field. The contours are 2 (dotted line), 4,8 and 16σ (solid lines) above the mean value (poissonian statistics). The location of our 8 candidates is also shown.

from each other (see upper panel of Fig. 2). This represents a projected separation of $50h_{50}^{-1}$ kpc, and we would thus see a close pair of primordial galaxies.

We have drawn the galaxy density map in the field. This is shown on Fig. 4, together with the location of all our high redshift candidates. As can be seen, the pair H1/H2 is located on the edge of an overdensity, which is significant at 16σ level. No other high redshift candidate is detected in the same area of the field, due to useless photometry, and they could belong to a very high redshift structure.

In the hypothesis that these objects are at redshifts around 4.6, and correcting the fact that we considered only 88 objects among the 352 that we detect in the apparent magnitude range [23.5, 25], we come to a projected density of 0.7 object per square arcminute. This value is very close to the one derived by Steidel et al. (1995) at redshifts around 3.2, thus involving no strong evolution of the projected density of galaxies between $z = 4.5$ and $z = 3.2$. We note however that, due to cosmological evolution, this leads to strong change in the physical density, but that Miralles & Pello (1998) have recently shown that the density of high redshift objects could be as high as 50 times higher than the one derived by Steidel et al. (1995)

3.2. The lower redshift candidates

Intermediate panel of Fig. 2 shows the images of object L3, which is likely to be a galaxy with redshift in the range $4.12 \leq z \leq 4.32$. Again the color-color plot ($F(4950)/F(4590)$ vs $F(6800)/F(5400)$ for this red-

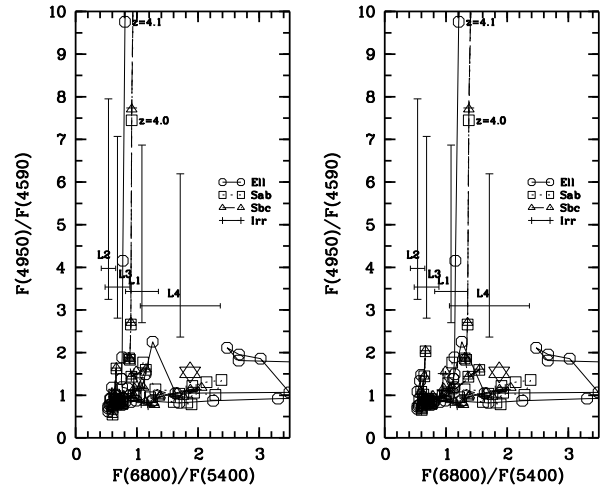


Fig. 5. Color-color diagram for the lower redshift candidates. $F(6800)$ denotes the flux in the R band, while $F(4950)$ and $F(4590)$ are the fluxes in the two bluer bands of the multiband filter. The location of our four candidates, with the 3σ error bars are also shown. Left diagram is for a high intergalactic transmission, right diagram for average value of the transmission. The star-like symbol shows the colors of an M type star

shift range, Fig. 5) shows that no lower redshift objects can reproduce the observed colors, and that the $F(4950)/F(4590)$ value alone can discriminate high redshift objects. The only possible exception is object L4, which has colors compatible at slightly more than 3σ with lower redshift ellipticals at $z = 0.2$ or $z = 0.7$.

3.2.1. Peculiar objects

This experimental setup also has the capability to bring out objects with other kinds of spectral feature, in particular emission lines. In our sample of faint galaxies, we have found one such object, labeled E1 in table 1. The flux in the intermediate band is about 3 times greater than in other bands (including the R band). It is thus likely that this object shows a strong emission line in the wavelength range 4855–5065 Å. Unfortunately, there is no way to distinguish between the various lines, and this object could either be a $\text{Ly}\alpha$ emitting object at $z \sim 3.1$, or a local dwarf object ($M_R \sim -18$) at $z \sim 0.33$ which shows strong O II emission.

Acknowledgements. This experiment has been made possible thanks to a strong support of the IGRAP. We also would like to thank E. Pelletier and G. Albrand for the realization of the very high transmission multi-band filters, as well as A. Baranne for doing all optical computations, and B. di Biagio and L. Castinel for the realization of the mechanical structure. We also thank H.H. Hippelein for kindly providing us with the CADIS field position and finding charts, A. Gilliotte for his essential help at the ESO-La Silla Optical Laboratory dur-

ing the observations, and H. Plana and P. Ambrocio-Cruz for their help during the observations. We thank V. Afanasiev, S. Dodonov and H. Hippelein for fruitful discussion. V. Le Brun is supported by a grant from the "Société de Secours des Amis des Sciences" of the Académie des Sciences de Paris

References

- Bertin E., Arnouts S., 1996, *A&AS* 117, 393
 Boulesteix J. et al., 1997, in preparation
 Bruzual G., Charlot S., 1993, *ApJ*, 405, 538
 Charlot S., Fall S., 1993, *ApJ*, 405, 538.
 De Propriis R., Pritchett C., Hartwick F., Hickson P. 1993, *AJ*, 105, 1243
 Driver S.P., Phillipps S., Davies J.I., Morgan I., Disney M.J., 1995, *MNRAS* 266, 155
 Franx M., Illingworth G.D., Kelson D.D., van Dokkum P.G., Tran K.-V., 1997, *ApJ* 485, L75, astro-ph/9704090
 Hammer F., Flores H., Lilly S. J., et al., 1997, *ApJ* 481, 49
 Hippelein H., Meisenheimer K., Thommes E., Fockenbrock R., Röser H., 1995, "New light on Galaxy Evolution", IAU Symp 171, Heidelberg, June 26-30, 1995.
 Hu, E., In S. D'Odorico, A. Fontana and E. Giallongo (Eds), "The Young Universe: Galaxy Formation and Evolution at Intermediate and High Redshift", ASP Conf. Series, astro-ph/9801170
 Koo D., Kron R., 1980, *PASP*, 92, 537
 Le Brun V., Bergeron J., Boissé P., Christian C., 1993, *A&A* 279, 31
 Madau P., 1995, *ApJ* 441, 18
 Metcalfe N., Fong R., Shanks T., Jones L.R., 1991, *MNRAS* 249, 498
 Miralles J.-M., Pello R., 1998, submitted to *ApJ*, astro-ph/9801062
 Parkes I., Collins C., Joseph R., 1994, *MNRAS*, 266, 983
 Schneider P., Schmidt M., Gunn J., 1991, *AJ*, 102, 837
 Smail I., Hogg D.W., Yan L., Cohen J., 1995, *ApJ* 449, L105
 Steidel C.C., Hamilton D., 1992, *AJ* 104, 941
 Steidel C.C., Hamilton D., 1993, *AJ* 105, 2017
 Steidel C.C., Pettini M., Hamilton D., 1995, *AJ* 110, 2519
 Stone R.P.S., 1977, *ApJ* 218, 767
 Thompson D., Djorgovski S., 1995, *AJ*, 110, 982
 Thompson D., Djorgovski S., Trauger J., 1995, *AJ*, 110, 963